Role of IL-4 in bone marrow driven dysregulated angiogenesis and age-related macular degeneration

Takashi Baba[1]*, Dai Miyazaki[1]*, Kodai Inata[1], Ryu Uotani[1], Hitomi Miyake[1], Shin-ichi Sasaki[1], Yumiko Shimizu[1], Yoshitsugu Inoue[1], Kazuomi Nakamura[2]

[1]Division of Ophthalmology and Visual Science, Faculty of Medicine, Tottori University, Yonago, Japan; [2]Division of Pathological Biochemistry, Department of Biomedical Sciences, Faculty of Medicine, Tottori University, Tottori, Japan

Abstract Age-associated sterile inflammation can cause dysregulated choroidal neovascularization (CNV) as age-related macular degeneration (AMD). Intraocular fluid screening of 234 AMD patients identified high levels of IL-4. The purpose of this study was to determine the functional role of IL-4 in CNV formation using murine CNV model. Our results indicate that the IL-4/IL-4 receptors (IL4Rs) controlled tube formation and global proangiogenic responses of bone marrow cells. CCR2$^+$ bone marrow cells were recruited to form very early CNV lesions. IL-4 rapidly induces CCL2, which enhances recruitment of CCR2$^+$ bone marrow cells. This in vivo communication, like quorum-sensing, was followed by the induction of IL-4 by the bone marrow cells during the formation of mature CNVs. For CNV development, IL-4 in bone marrow cells are critically required, and IL-4 directly promotes CNV formation mainly by IL-4R. The IL-4/IL-4Rα axis contributes to pathological angiogenesis through communications with bone marrow cells leading to retinal degeneration.

*For correspondence:
babatakashi8@gmail.com (TB);
miyazaki-ttr@umin.ac.jp (DM)

Introduction

Age-related macular degeneration (AMD) is a neurodegenerative disorder which develops in elderly individuals and is a major cause of visual impairments in developed countries. In the early stages of AMD, lipoprotein deposits called drusen accumulate in the subretinal space between the photoreceptors and retinal pigment epithelium (RPE). Drusen are associated with the degeneration of the RPE which then leads to a dysfunction or loss of the photoreceptors. Choroidal (CNVs) develop in the subretinal space, and the CNVs lead to degeneration of the photoreceptor cells, infiltration by inflammatory cells, activation of microglia, and ganglion cell loss (*Beck et al., 2016*; *Copland et al., 2018*).

The pathology of AMD is coupled with senescence-associated para-inflammation, which is characterized by the secretion of IL-6, IL-8, CCL2, and CX3CL1 (*Sasaki et al., 2010*). Of these, CCL2 plays an important role in recruiting bone marrow cells, monocytes, and macrophages to the ocular neovascularizations. In this disease process, the bone marrow plays an important role by supplying new vascular endothelial cells and macrophages to the retina (*Gao et al., 2016*; *Zhou et al., 2017*). Thus, the bone marrow plays a key role in the repair of damaged tissues.

The M1 macrophages are functionally classified as pro-inflammatory, and the M2 macrophages are classified as anti-inflammatory, and both types are recruited to damaged tissues. The M2 macrophages are induced by IL-4, and it has been suggested that they have disease-regulating functions as opposed to the M1 macrophages (*Zhou et al., 2017*).

The concept of IL-4 as a regulatory and neuroprotective cytokine is supported by the findings in other neurodegenerative diseases including Alzheimer's disease (*Kiyota et al., 2010*) and

Parkinson's disease (*Chitnis and Weiner, 2017*; *Zhao et al., 2006*). Moreover, IL-4 is known to be a potent inhibitor of angiogenesis (*Haas et al., 2006*; *Volpert et al., 1998*), and thus may prevent pathological angiogenesis in eyes with AMD.

The purpose of this study was to determine whether bone marrow cells and IL-4 protect the photoreceptors from neurodegeneration, and whether they play regulatory roles in eyes with g AMD. To accomplish this, we first determined the concentration of IL-4 and other inflammatory cytokines in the aqueous humor of the eyes of AMD patients (*Sasaki et al., 2012*). We then determined whether IL-4 and bone marrow cells play roles in protecting the eye from abnormal angiogenesis. This was done by functional assays and global transcriptional profiling of bone marrow cells derived from endothelial progenitor cells (EPC).

Results

Increased levels of IL-4 in aqueous humor of eyes with AMD and clinical subtypes of AMD

We first examined the levels of IL-4 and related cytokines in the aqueous humor of human eyes with AMD. To accomplish this, aqueous humor was collected from the eyes of 234 patients with clinically-diagnosed AMD and impaired central vision and 104 normal subjects undergoing routine cataract surgery. The mean age of the patients with AMD was 74.1 ± 0.6 years, and it was 74.9 ± 1.0 years for the normal subjects. The results showed that the AMD patients had significantly higher levels of IL-4 in their aqueous than in normal subjects (*Table 1*, *Table 2*). In contrast, there was no significant elevation of IL-13.

We next examined whether the IL-4 levels were significantly associated with the different subtypes of AMD. The results showed that the level of IL-4 was significantly higher in the three clinical subtypes of AMD, for example, typical AMD, polypoidal choroidal vasculopathy (PCV), and retinal angiomatous proliferation (RAP). The degree of elevation of IL-4 (quintile) had the highest relative-risk ratio of 2.5 for RAP (p=0.001, logistic regression analysis after age adjustments), followed by 2.1 for typical AMD (p=0.000) and 1.7 for PCV (p=0.000) (*Table 2*).

IL-4 induction in murine experimental choroidal neovascularization

The level of IL-4 expression was evaluated in a murine laser-induced CNV model to determine whether IL-4 is associated with subretinal neovascularization. First, we assessed whether the mRNA of IL-4 was induced in the CNV lesions. Our results showed that the mRNA of IL-4 was elevated and peaked at 3 days after the laser exposure and then decreased (*Figure 1a*). The mRNA of IL-4Rα also had similar induction kinetics. The mRNA of CCR2, a myeloid cell recruitment marker, was elevated, and the elevation preceded the mRNA of IL-4 induction by peaking at 1 day. The mRNA of CD11b gradually increased after the exposure.

To examine the spatial expression of IL-4, we examined the CNV lesions by immunohistochemistry. Three day after the laser exposure, the IL-4-expressing cells were observed along the margins of the lesions and were present more centrally on day 7 (*Figure 1b*). The IL-4-expressing cells were largely CD11b^{+}, and they were considered to be myeloid- or macrophage-lineage cells. The kinetics of Iba1-, CCL2-, and CD11b-positive cells after laser exposure was consistent with that of the mRNA induction (*Figure 1—figure supplement 1*).

We then examined which type of lineage cells can produce the CCL2 as an early recruitment signal for myeloid cells. Our results showed that the CCL2 was mainly associated with iba1-positive

Table 1. Increase of IL-4 concentration in aqueous humor of eyes with age-related macular degeneration.

Cytokines (pg/ml)	Control (n = 104)	age-related macular degeneration (n = 234)	*P* value
IL-4	0.3 ± 0.1	0.9 ± 0.1	p=0.0000
IL-13	3.8 ± 0.7	5.2 ± 0.7	NS

Two-tailed t test; Mean ± standard error of the means (SEMs).

Table 2. Association of IL-4 concentration in aqueous humor with subtype of age-related macular degeneration.

| | N | Relative risk ratio | | Relative risk ratio | |
		IL-4 (quintile)	P value	IL-13 (quintile)	P value
Control	104	-	-	-	-
Typical AMD	33	2.11 ± 0.33	0.000	2.09 ± 0.39	0.000
Polypoidal choroidal vasculopathy (PCV)	78	1.70 ± 0.17	0.000	1.39 ± 0.15	0.002
Retinal angiomatous proliferation (RAP)	11	2.46 ± 0.69	0.001	1.48 ± 0.37	0.11

Multinomial logistic regression analysis after age adjustment; Mean ± standard error of the means (SEMs).

retinal microglial cells (*Figure 1c*). The microglial cells migrated to surface of the CNV (*Figure 1—video 1*). This indicated that they were the initial stimulators. Thus, IL-4 expressions followed by myeloid cell activation were early events acting at the inductive phase of the CNV formation.

Requirement of IL-4 in inductive phase of choroidal neovascularization

The kinetic observations suggested that IL-4 appeared in the inductive phase of CNV formation. To determine whether IL-4 had inhibitory or stimulatory effects on the pathological angiogenesis, mice were laser-treated to induce the formation of CNVs, and IL-4 was injected intravenously on day 0 and day 3 during the inductive phase. The IL-4 significantly exacerbated the CNV formation in a dose dependent way (*Figure 2a*).

It is known that IL-4 generally signals through IL-4Rα which is also a ligand of IL-13. Therefore, we also tested whether IL-13 had any stimulatory effect on CNV formation. Our results showed that a systemic administration of IL-13 in the inductive phase had no significant effect on CNV formation.

To examine the role of IL-4 in the inductive phase of CNV development in more detail, laser-treated mice were injected intravenously with an anti-IL-4 antibody on day 0 and day 3 to try to inhibit the expression of IL-4 (*Figure 2b*). Consistent with the effects of IL-4 administration, an IL-4 blockade significantly reduced the size of the CNV. In contrast, a block of IL-13 by an antibody injection had no significant effect on the CNV formation.

We next evaluated the contribution of IL-4 to the formation of CNVs using *Il4*-deficient mice (*Figure 2c*). Consistent with the outcomes of the anti-IL-4 antibody exposure, *Il4*-deficient mice were significantly impaired in CNV formation which supports our finding that IL-4 is involved in the inductive phase of CNV. To confirm that IL-4 contributed to the CNV formation with canonical signaling by IL-4Rα in more detail, *Il4ra*-deficient mice were tested for CNV formation. *Il4ra*-deficiency impaired the CNV formation significantly (*Figure 2d*).

Next, we evaluated role of the IL-13 receptors as alternative receptors of IL-4. IL-13R is composed of IL-4Rα and IL-13Rα1. When IL-13Rα1-deficient mice were tested for CNV formation, no significant impairment was observed.

Incorporation of circulating angiogenic cells and bone marrow-derived cells into CNV lesion

It has been shown that bone marrow cells are recruited into the CNV lesions during the inductive phase of CNV formation (*Gao et al., 2016*). Therefore, we examined the roles played by bone marrow-derived cells in CNV formation using bone marrow chimeric mice. Bone marrow chimeric mice were generated by reconstitution with a GFP transgenic mice-bone marrow, and they were evaluated for laser-induced CNV formation (*Figure 2e*).

Recruitment of GFP[+] bone marrow-derived cells (green) peaked at 3 days after irradiation. Thus, bone marrow-derived cell recruitment also contributed to the inductive phase process. Bone marrow-derived cells in this phase were CD11b^{+} lineage, and they were positive for CCL2. These bone marrow cells did not express iba1 and were morphologically distinct from microglial cells. This suggested that these cells will amplify the recruitment of CCR2^{+} lineage cells (*Figure 2—figure supplement 1*). Seven days after irradiation, bone marrow-derived cells were incorporated into structures formed by CD31^{+} endothelial cells (*Figure 2—video 1*).
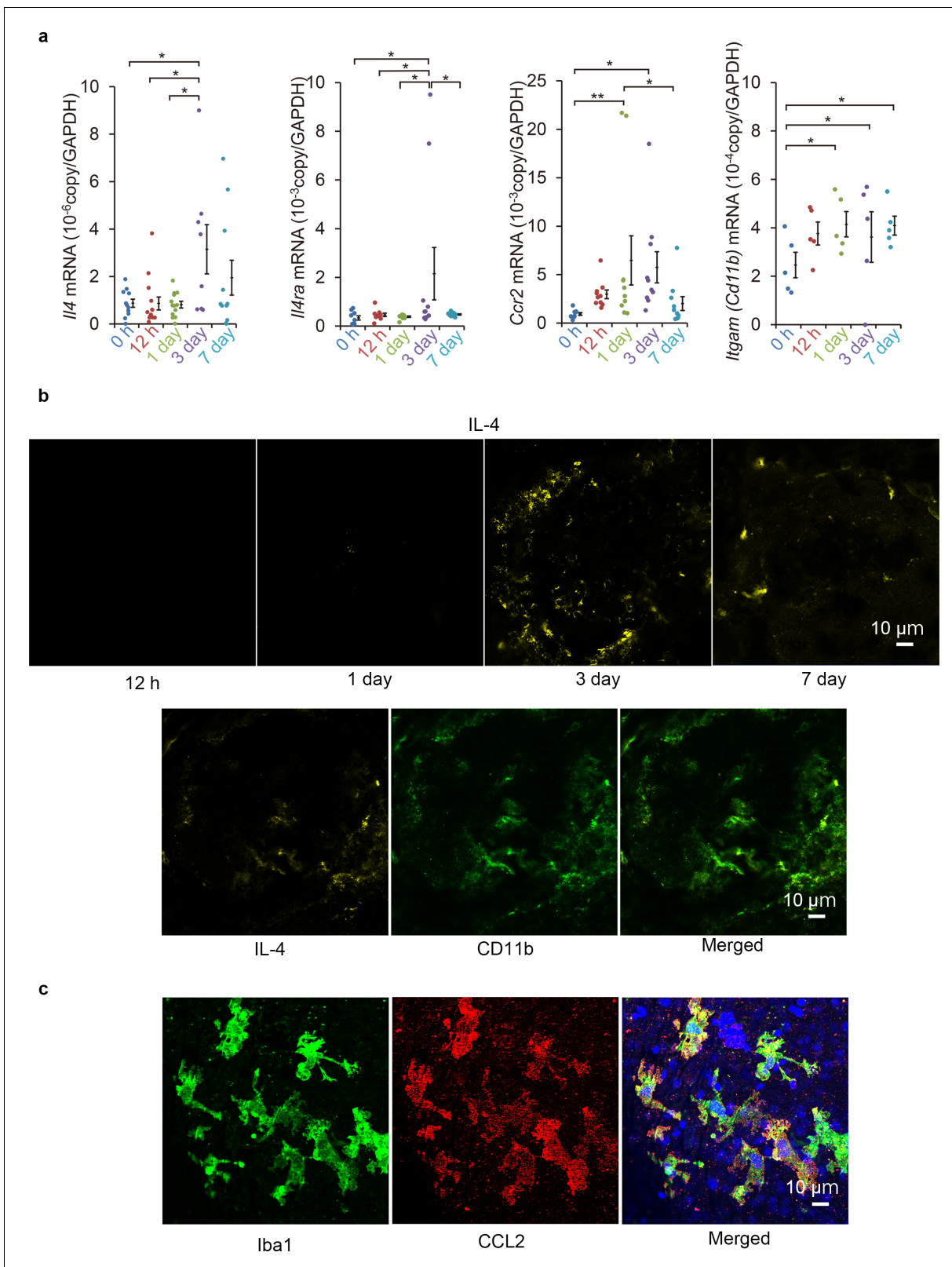
Figure 1. Induction of *Il4* and *Ccl2* in laser-exposed retinas and choroids of mice. (a) Induction kinetics of the mRNAs of IL-4, IL-4Rα, CCR2, and CD11b. The induction of *Ccl2* peaked at 1 day after the exposure followed by the peak induction of *Il4* and *Il4ra*. (n = 4–14 eyes/group). (b) Kinetics of IL-4-expressing cells by immunohistochemical analyses. IL-4 expressing cells (yellow) accumulated along the margin of laser treated area at 3 days and then move inwards. The IL-4-expressing cells (yellow) were mainly CD11b positive (green) in laser treated areas at 3 days. (c) Localization of CCL2

Figure 1 continued on next page

Figure 1 continued

expression in retinal tissue by immunohistochemistry. CCL2 induction is observed at 1 day after treatment, and CCL2-positive cells (red) are colocalized with the iba1-positive microglial cells (green). The nuclei were stained by TO-PRO-3 iodide (blue). Scale 10 μm. *p<0.05, **p<0.01. ANOVA with post hoc test and linear mixed-effects regression analysis.

The online version of this article includes the following video, source data, and figure supplement(s) for figure 1:

Source data 1. Induction kinetics of the mRNAs of IL-4, IL-4Rα, CCR2, and CD11b.

Figure supplement 1. Kinetics of IL-4-expressing cells by immunohistochemical analyses in retinal flat mount.

Figure 1—video 1. Localization of bone marrow-derived cells and microglial cells in the retinal tissue of GFP bone marrow chimeric mouse in 3D rendering at 3 days after laser irradiation.

https://elifesciences.org/articles/54257#fig1video1

Two weeks after laser exposure, CNVs were formed as clusters of isolectin-positive vascular endothelial cells (red; *Figure 2e*). In the CNV lesion, bone marrow-derived cells (green) were localized to isolectin-positive vascular endothelial cells and CD31$^+$ endothelial cells. The co-localization of the marrow-derived cells with CD31$^+$ endothelial cells indicated that the bone marrow-derived cells may be able to differentiate into endothelial cells. IL-4-positive cells (yellow) were distributed at the margins of the CNVs and precisely matched the bone marrow-derived cells (green). The IL-4Rα-positive cells (cyan) in the CNV, partly overlapped the bone marrow-derived cells.

Profiles of angiogenic mRNAs of endothelial progenitor cells

These findings suggested that the IL-4 from bone marrow-derived vascular endothelial cells played disease-promoting roles in CNV formation, and they were not anti-angiogenic. To confirm this, we examined how IL-4 affected the differentiation of vascular endothelial progenitor cells (EPC) from bone marrow cells. To do this, bone marrow cells were cultured for differentiation to late EPCs for 2 weeks and exposed to IL-4. We then screened for the induction of angiogenesis-related mRNAs, including *Ccl2*, *Vegf*, VEGF receptors (*Kdr*, *Flt4*), angiopoietin-1 (*Angpt1*), endothelin receptor (*Ednrb*), thrombin receptors (*F2r*, *F2rl1*), P-selectin (*Selp*), and vascular endothelial cadherin (*Cdh5*) (*Figure 3a*, *Figure 3—figure supplement 1*, *Figure 3—figure supplement 2*). Of these, *Ccl2* and *Flt1* were significantly induced in a dose dependent manner after IL-4 exposure. *Kdr* and *Flt4* were not induced.

We also examined whether mature vascular endothelial cells can induce comparable transcriptional responses. When retinal microvascular cells were tested for their effect on IL-4 by real-time reverse transcription PCR (RT-PCR), IL-4 was found to stimulate the induction of *Ccl2/Flt1* (*Figure 3b*).

An upregulation of the translation of CCL2 and VEGFR-1 in EPCs was confirmed by ELISA. IL-4-exposed EPCs had a significant increase in the secretion of CCL2 (p=0.000) and VEGFR-1 (p=0.000) after 24 hr exposure to IL-4 (*Figure 3—figure supplement 2*).

We next examined how IL-4Rα and IL-13Rα1 contributed to the induction of *Ccl2* and *Flt1* in EPCs by IL-4, IL-13, and VEGF. Both IL-4 and IL-13 significantly induced *Ccl2* and *Flt1* in EPCs (*Figure 3*). However, VEGF did not significantly induce *Ccl2* and *Flt1*. When IL-4Rα was inhibited by an anti-IL-4Rα antibody, IL-4 failed to stimulate the EPCs from inducing the expression of *Ccl2* and *Flt1* (*Figure 3a*).

To determine the contribution of IL-4Rα to CNV formation, we examined the effect of *Il4ra* deficiency. EPCs from *Il4ra*-deficient mice did not induce *Ccl2* and *Flt1* in response to IL-4 or IL-13 (*Figure 3c*).

We also examined the contribution of IL-13Rα1 to the formation of CNVs. When *Il13ra1*-deficient EPC mice were stimulated by IL-4, *Ccl2* and *Flt1* were still induced (*Figure 3d*) indicating that IL-13Rα1 was not necessary for IL-4 stimulation. When *Il13ra1*-deficient EPC mice were stimulated with IL-13, *Ccl2* and *Flt1* were not induced. Collectively, these findings indicate that IL-4Rα is the major receptor for IL-4 to induce the expression of CCL2 and VEGFR-1, and the IL-13Rα1 can substitute for their induction mainly through IL-13.

We next examined whether the *Ccl2* and *Flt1* induction by IL-4 required intrinsic IL-4-mediated differentiation. The results indicated that the EPCs of *Il4*-deificient mice still induced IL-4 and the IL-13-mediated *Ccl2* and *Flt1* induction (*Figure 3e*).
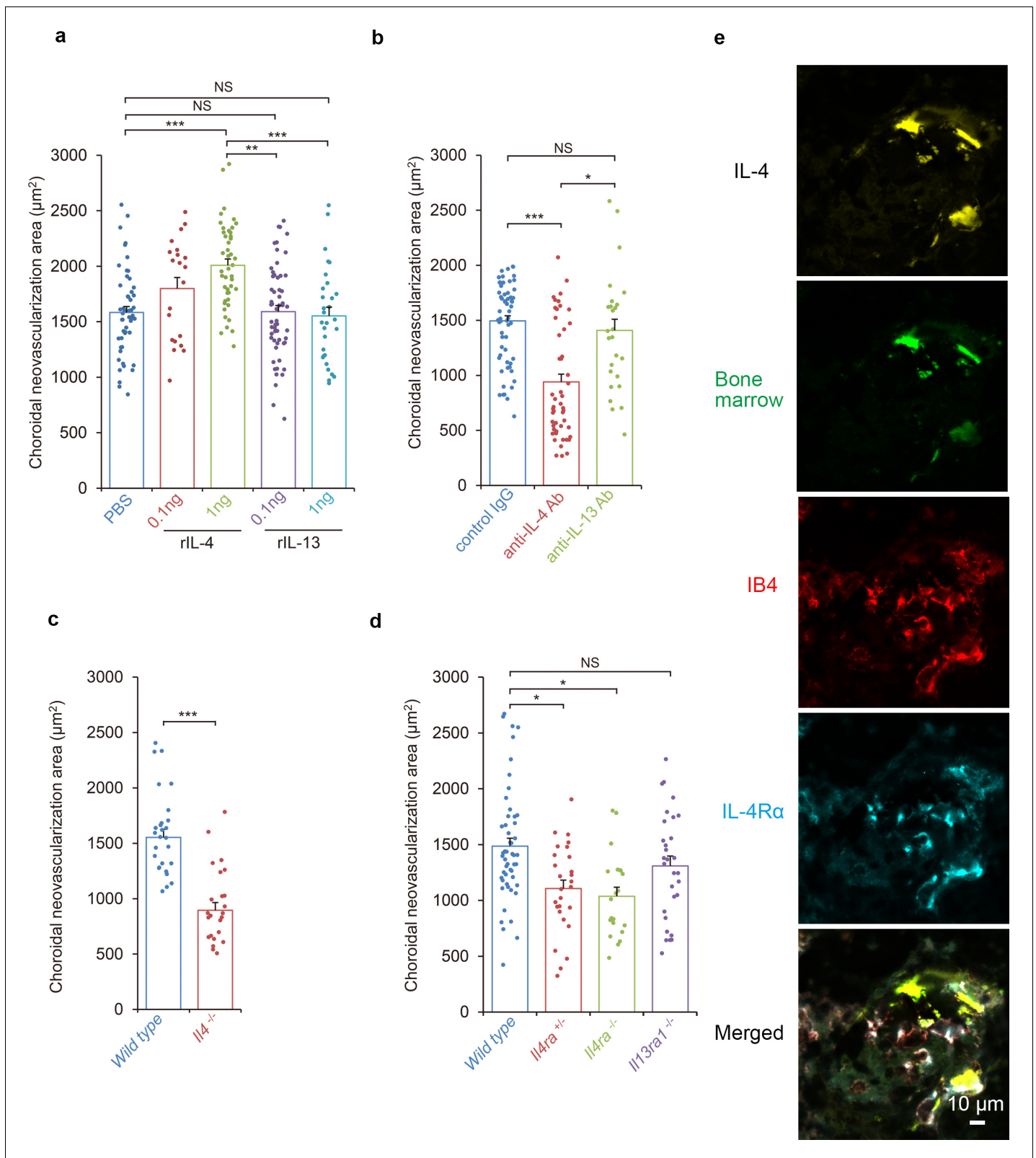
Figure 2. Requirements of IL-4/IL-4Rα in the inductive phase of choroidal neovascularization (CNV). (a) Effect of systemic administration of recombinant murine IL-4 (rIL-4) or recombinant IL-13 (rIL-13) in the inductive phase in a CNV model. (n = 7–19 eyes/group). (b) Inhibitory effect of systemic administration of anti-IL-4 antibody in the inductive phase of CNV formation. (n = 7–20 eyes/group). (c) Impaired CNV development in *Il4* deficient mice. CNV development is significantly impaired in *Il4*$^{-/-}$ mice compared to *wild type*. (n = 8–9 eyes/group). (d) Impaired CNV development by IL-4

Figure 2 continued on next page

Figure 2 continued

receptors deficiency. CNV development is significantly impaired in *Il4ra*$^{-/-}$ and *Il4ra*$^{+/-}$ mice compared to *wild type*. This impairment is more marked in the homozygotes. CNV development is not impaired for *Il13ra1*$^{-/-}$ mice. (n = 7–17 eyes/group) (e) Bone marrow chimeric mice reconstituted with *GFP* transgenic bone marrow cells that were exposed to laser to induce CNVs. The CNV lesions after 14 days were analyzed for lineage cell markers by immunohistochemistry. CNVs are formed as clusters of isolectin IB4-positive vascular endothelial cells (red). Bone marrow-derived cells (green) were co-localized with isolectin-positive vascular endothelial cells. IL-4 positive cells (yellow) are distributed at the margins of the CNVs and precisely match the location of the bone marrow-derived cells (green). IL-4Rα-positive cells (cyan) partly overlapped the bone marrow-derived cells, and precisely match the location of the vascular endothelial cells in the CNV lesion. *p<0.005, **p<0.001, ***p<0.0005. Nested ANOVA with post hoc test. Scale 10 μm.

The online version of this article includes the following video, source data, and figure supplement(s) for figure 2:

Source data 1. Requirements of IL-4/IL-4Rα in the inductive phase of CNV.

Figure supplement 1. Kinetics of IL-4, IL-4Rα, CCR2 and CD11b-expressing cells and GFP-positive bone marrow derived cells determined by immunohistochemical analyses.

Figure 2—video 1. Localization of bone marrow-derived cells and endothelial cells in the retinal tissue of GFP bone marrow chimeric mouse in a 3D rendering 7 days after laser irradiation.

https://elifesciences.org/articles/54257#fig2video1

Tube formation by endothelial progenitor cells and vascular endothelial cells stimulated by IL-4

To confirm a vasculogenic property of IL-4, mature vascular endothelial cells were assessed for tube formation on Matrigel-coated plates (*Figure 4a*). When murine retinal microvascular endothelial cells were tested for tube formation by IL-4 or VEGF, both stimulated significant tube formation (*Figure 4a*). Anti-IL-4 and IL-4Rα antibodies abolished the IL-4-induced tube formation.

We next confirmed the effects of IL-4 using human retinal cells (*Figure 4a*). IL-4 exposure stimulated tube formation by human retinal vascular endothelial cells, and anti-IL-4 and IL-4Rα antibodies blocked this effect.

Next, EPCs were examined for IL-4-mediated tube formation. Murine bone marrow cells were cultured under conditions appropriate for the differentiation of EPCs and were tested for tube formation. For the *wild type* bone marrow cells, IL-4 significantly stimulated tube formation by the EPCs (*Figure 4bc*). This IL-4-induced tube formation was blocked when the bone marrow cells were deficient of *Il4ra*. However, the inhibition of the VEGF receptor tyrosine kinase or VEGF receptor 2 did not significantly inhibit tube formation (*Figure 4b*). This indicated that this IL-4 effect was independent of canonical VEGF signaling.

The IL-4-induced tube formation was blocked when the cells were deficient of *Il4* but not by *Il13ra1* deficiency (*Figure 4c*). IL-13 also stimulated tube formation by bone marrow-derived EPCs. This response was abolished when the bone marrow cells were deficient in *Il4* and *Il13ra1*. These findings further confirmed the roles of IL-4 as a differentiation and vasculogenic factor which signaled mainly through IL-4Rα. The results also indicated that IL-13Rα1 could serve as an alternative receptor.

IL-4Rα-dependent transcriptional networks of tube forming endothelial progenitor cells from bone marrow cells

The results suggested that IL-4 also served as a differentiation factor for cells of endothelial lineage. To characterize the vasculogenic roles of IL-4 for bone marrow cells, the mRNA of tube-forming EPCs were extracted and examined by network analysis. Analysis of the functions of IL-4-stimulated EPCs indicated significant association with the homing of the cells (Z score = 2.798, p=8.3 $\times$ 10^{-5}), angiogenesis (Z score = 2.781, p=1.8 $\times$ 10^{-4}), activation of macrophages (Z score = 2.731, p=1.0 $\times$ 10^{-5}), and recruitment of myeloid cells (Z score = 2.606, p=2.8 $\times$ 10^{-10}) (*Figure 4—figure supplement 1*).

Requirements of IL-4 in bone marrow-mediated choroidal neovascularization

The results suggested that the IL-4 and IL-4Rα interactions contributed to the pathological angiogenesis of bone marrow-derived EPCs. To examine how bone marrow-derived cells contributed to IL-4-stimulated CNV formation, bone marrow chimeric mice were constructed on a *wild type* background of *Il4*- or *Il4ra*-deficient mice (*Figure 5*).
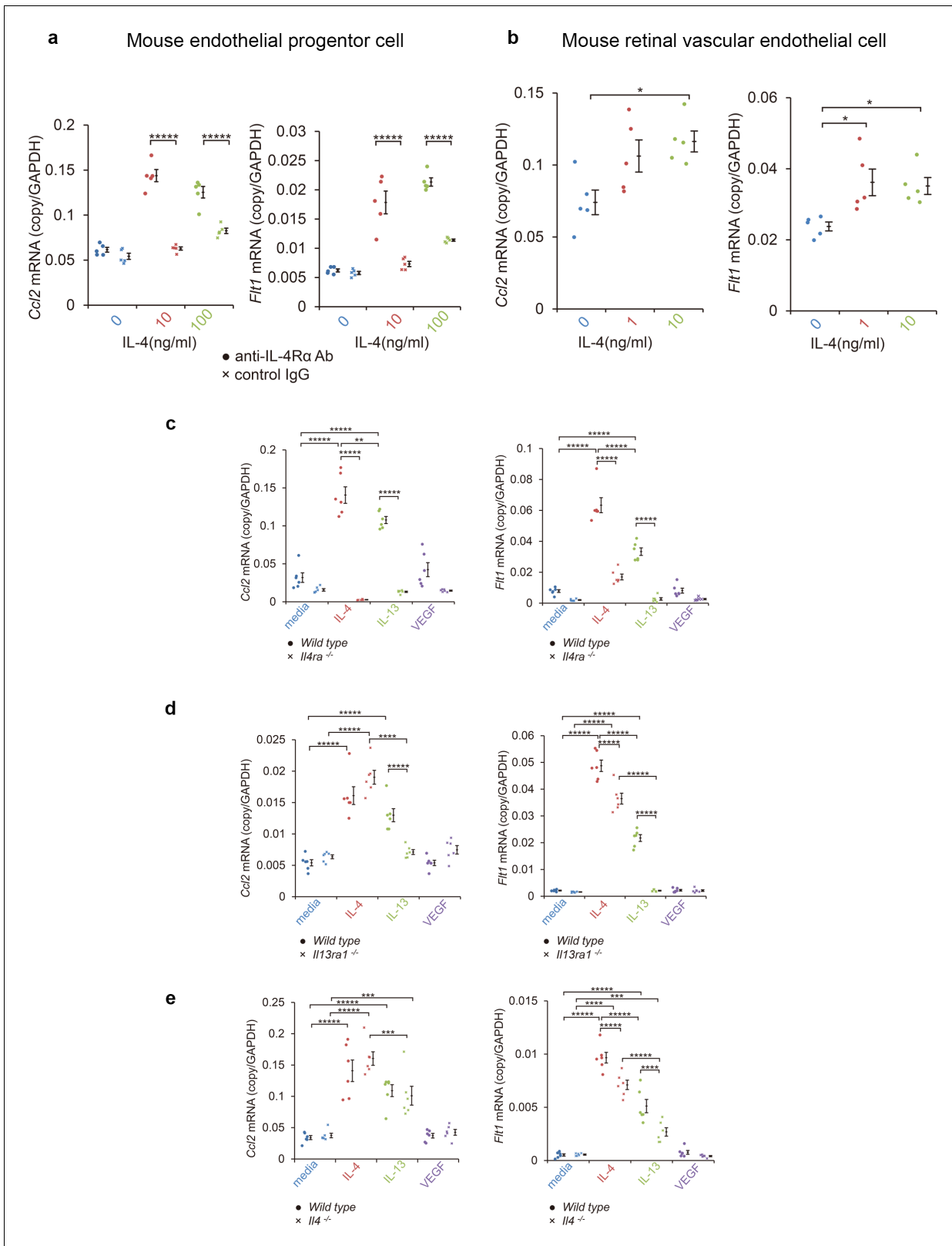
Figure 3. Induction of *Ccl2* and *Flt1* in bone marrow-derived endothelial progenitor cells (EPC) and retinal vascular endothelial cells by IL-4. (a) Induction of *Ccl2* and *Flt1* in bone marrow-derived endothelial progenitor cells by murine IL-4. IL-4 stimulated bone marrow-derived EPCs induced *Ccl2* and *Flt1* in a dose dependent manner. This induction is abolished by anti-IL-4Rα antibody. (n = 5/group). (b) Induction of *Ccl2* and *Flt1* in retinal vascular endothelial cells by IL-4. IL-4 stimulated vascular endothelial cells to express *Ccl2* and *Flt1* in a dose dependent manner. (n = 5/group). (c)
Figure 3 continued on next page

Figure 3 continued

Inhibition of IL-4/IL-13-mediated *Ccl2* and *Flt1* induction in EPCs by *Il4ra* deficiency (n = 6/group). IL-4 and IL-13 exposure induced *Ccl2* and *Flt1* in EPCs. This induction is not present in the EPCs of *Il4ra*^{-/-} mice. (d) Inhibition of IL-13-mediated *Ccl2* and *Flt1* induction in EPCs by *Il13ra1* deficiency (n = 6/group). The IL-13-induced the expression of *Ccl2* and *Flt1* is significantly reduced in *Il13ra1*^{-/-} EPCs of mice. IL-4-induced *Ccl2* and *Flt1* mRNA is not affected in *Il13ra1*^{-/-} EPCs of mice. (e) EPCs of *Il4* [-/-] mice respond to induce *Ccl2*/*Flt1* mRNA by IL-4/IL-13 exposure. (n = 6/group). *p<0.05, **p<0.01, ***p<0.005, ****p<0.0001, *****p<0.0005. ANOVA with post hoc test.

The online version of this article includes the following source data and figure supplement(s) for figure 3:

Source data 1. Induction of *Ccl2* and *Flt1* in bone marrow-derived EPC and retinal vascular endothelial cells by IL-4.
Figure supplement 1. Profile of angiogenic mRNAs of bone marrow-derived endothelial progenitor cells (EPCs) after IL-4 exposure.
Figure supplement 1—source data 1. Profile of angiogenic mRNAs of bone marrow-derived EPCs after IL-4 exposure.
Figure supplement 2. The CCL2 and VEGFR-1 protein levels in bone marrow-derived EPCs after IL-4 exposure.
Figure supplement 2—source data 1. The CCL2 and VEGFR-1 protein levels in bone marrow-derived EPCs after IL-4 exposure.

The *Il4*-deficient mice with *Il4*^{-/-} bone marrow developed the smallest size CNVs of all the chimeric mice. This impaired CNV formation was completely restored by the transplantation of bone marrow cells from *wild type* mice. This indicated the crucial role played by IL-4 in bone marrow cells. In contrast, *wild type* mice with *Il4*^{-/-} bone marrow were still impaired for CNV formation which indicated that the host resident cell-derived IL-4 is limited in this activity (*Figure 5a*).

Consistent with the results shown in *Figure 2*, *Il4ra*-deficient mice with *Il4ra*^{-/-} bone marrow cells were impaired in the formation of CNVs. This impairment was restored by the transplantation of *wild type* bone marrow cells (*Figure 5a*).

We next examined whether IL-4 secreting cells were recruited from bone marrow or were derived from the host. To do this, we conducted immunohistochemical analyses of *Il4*-deficient mice reconstituted with *wild type* bone marrow cells. The results showed IL-4- and IL-4Rα-positive cells were present in the CNV lesion (*Figure 5b*; *Figure 5—figure supplement 1*). The IL-4-positive cells precisely matched the bone marrow-derived cells (green). In contrast, the IL-4Rα positivity partly overlapped with that of the bone marrow-derived cells. This indicated that bone marrow-derived cells are the major producer of IL-4, and bone marrow-derived cells and resident cells in the CNV via IL-4Rα recognized their signals.

To summarize, interactions of IL-4/IL-4Rα interactions with bone marrow cells are required for pathological CNV formation.

Discussion

Our results showed that IL-4 played a crucial role in the pathogenesis of CNVs by directing the migration and activating the angiogenic bone marrow cells. IL-4 is the canonical Th2 cytokine and is secreted by an array of inflammatory cells including macrophages, monocytes, and activated retinal pigment epithelial cells (*Leung et al., 2009*). IL-4 is also recognized as a neuroprotective cytokine, and its action is not limited to the retina (*Adão-Novaes et al., 2009*). In axotomized retinas, the retinal ganglion cells are severely damaged by nitric oxide synthesis by activated glial cells. IL-4 significantly increases the survival of retinal ganglion cells, and prevents neurodegeneration caused by glial cell activation (*Koeberle et al., 2004*). In the thapsigargin-induced rod photoreceptor cell death model, IL-4 can completely block the death of the photoreceptors (*Adão-Novaes et al., 2009*). During the differentiation of the retina, IL-4 modulates the proliferation of the retinal cells and promotes photoreceptor differentiation (*da Silva et al., 2008*). In addition, a number of studies have shown that IL-4 can inhibit the death of photoreceptors and RGCs.

IL-4 is a multifaceted cytokine and is known to have anti-angiogenic capabilities. IL-4 inhibits tumor growth by inhibiting angiogenesis (*Volpert et al., 1998*) and also blocks corneal neovascularization induced by basic fibroblast growth factor. Thus, IL-4 can function as an anti-inflammatory cytokine and prevent neuronal death and angiogenesis. However, such properties of IL-4 appear to be context dependent.

We found that the IL-4 level was significantly elevated in the aqueous humor of patients with AMD (*Table 1*, *Table 2*; *Sasaki et al., 2012*). Together with this, our analyses of the bone marrow cells and chimeric mice supports the idea that elevations of IL-4- and IL-4 receptor-bearing cells are associated with the development of abnormal vessels in the lesions of eyes with AMD.
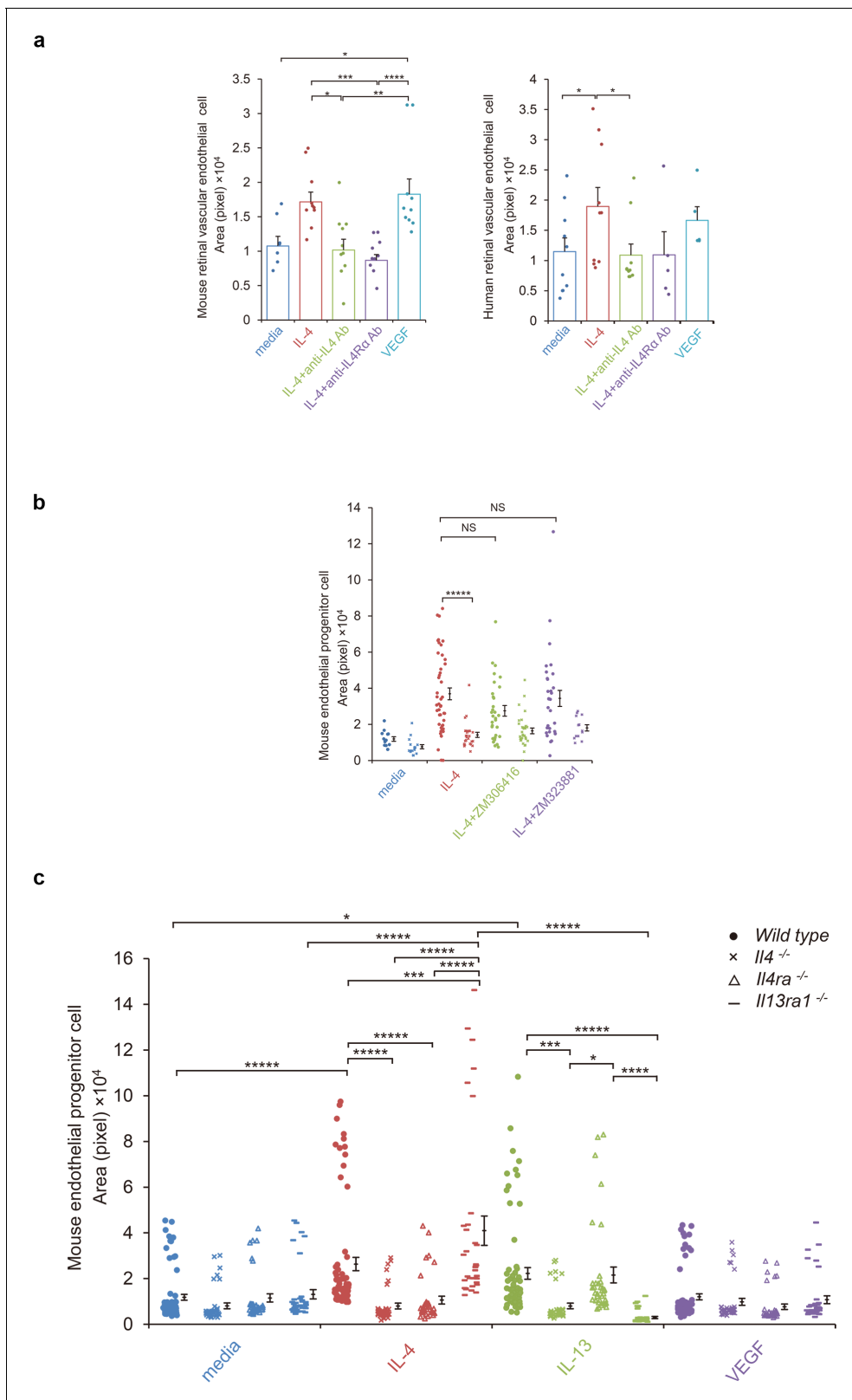
Figure 4. IL-4-induced tube formation in endothelial progenitor cells (EPCs) and retinal vascular endothelial cells. (**a**) IL-4-induced tube formation of retinal vascular endothelial cells. Human and murine IL-4 exposure (10 ng/ml) significantly stimulated tube formation of human and murine retinal microvascular endothelial cells in vitro, respectively. Anti-IL-4 or IL-4Rα antibodies abolished the IL-4 induced-tube formation. VEGF exposure (10 ng/ml) also stimulated tube formation. (n = 7–10/group). (**b**) IL-4-induced tube formation in bone marrow-derived EPCs. IL-4 exposure (10 ng/ml)

Figure 4 continued on next page

significantly stimulated tube formation of EPCs. The IL-4-induced tube formation was significantly reduced in EPCs from $Il4ra^{-/-}$ mice but was not affected by inhibition of VEGF receptor tyrosine kinase (ZM 306416) or VEGFR-2 (ZM 323881) (n = 13–45/group). (c) Requirements of IL-4 for tube formation response of EPCs. IL-4 (10 ng/ml) and IL-13 (10 ng/ml) induced tube formation of bone marrow-derived EPCs. These actions were abolished in the EPCs from $Il4^{-/-}$ bone marrow cells. EPCs from $Il4ra^{-/-}$ mice did not respond to IL-4, however they responded to IL-13 by tube formation. EPCs from $Il13ra1^{-/-}$ mice did not respond to IL-13 but responded to IL-4 by tube formation. (n = 35–72/group). *p<0.05, **p<0.01, ***p<0.005, ****p<0.001, *****p<0.0005. ANOVA with post hoc test and linear mixed-effects regression analysis.

The online version of this article includes the following source data and figure supplement(s) for figure 4:

Source data 1. IL-4-induced tube formation inEPCs and retinal vascular endothelial cells.

Figure supplement 1. IL-4Rα-mediated transcriptional networks of bone marrow-derived EPCs.

Figure supplement 1—source data 1. IL-4Rα-mediated transcriptional networks of bone marrow-derived EPCs.

Although the IL-4/IL-4Rα axis appears neuroprotective in the retina, retinal injury requires a recruitment or activation of cells with regenerative properties for its repair. The bone marrow cells are a major supplier of mesenchymal stem cells and hematopoietic stem cells. However, abnormally activated bone marrow cells by IL-4 in the retina promote pathological angiogenic responses.

To explain the dysregulated repair process after organ damage, the concept of cell level and organ level quorum sensing has been recently proposed (*Antonioli et al., 2018*). Quorum sensing was originally proposed as a phenomenon of bacterial cells, and it was described as a mechanism that senses the environment and integrity of a population of cells. Hair follicle injury sensed by a macrophage-mediated circuit via CCL2 is a well-known example of quorum sensing at the organ level (*Chen et al., 2015*; *Feng et al., 2017*). The quorum sensing circuit mediated by microglia-derived CCL2 also appears to operate in new vessel formation in the retina together with a late IL-4 modulator.

We observed the presence of CD11b in the CNV lesions at 12 hr which would indicate that monocyte/macrophage cells had arrived soon after the beginning of the CNV. In contrast, the induction of IL-4 and IL-4 receptors was delayed and peaked at 3 days (*Figure 1*). CCL2 recruits circulating mononuclear cells from the bone marrow, and the retinal pigment epithelial cells and microglial cells are the major sources of the CCL2 cells in the retina (*Feng et al., 2017*). Thus, the monocyte/macrophage recruiting signal, including CCL2, appears to be the first signal in the formation of CNVs.

It was reported that CCL2 is involved in the formation of retinal neovascularization (*Sennlaub et al., 2013*; *Yoshida et al., 2003*). However, the CCL2/CCR2 signals recruit a heterogeneous collection of monocyte/macrophage lineage cells and presumably do not determine their fate (*Grochot-Przeczek et al., 2013*; *Pearson, 2010*).

Bone marrow-derived cells and macrophages are critical contributors to retinal and choroidal neovascularization (*Gao et al., 2016*; *Zhou et al., 2017*). Higher levels of M1 than M2 type mRNAs were observed in advanced stage AMD patients (*Cao et al., 2011*). The M1 macrophages counteract the M2 type by the secretion of interferon-γ. Based on this, the M2 macrophages were considered to play a regulatory role in CNV formation. Consistent with this, Wu et al showed that the M2 type cytokine, IL-4, and conditioned macrophages become the regulatory phenotype to suppress the disease processes (*Wu et al., 2015*). However, the M1 types of IFNAR1+ macrophages have been reported to be protective in laser-induced CNV (*Lückoff et al., 2016*). Thus, the M1/M2 paradigm does not clearly explain how abnormal vessels are formed in AMD lesions or the CNVs of the model mice.

Wu et al also showed a contradictory role of IL-4 for CNV formation (*Wu et al., 2015*). This was shown using vitreous injection of IL-4 at very high concentration (600 ng/ml). This may cause toxic damage to endothelial cells or recruited cells which may not reflect physiological role of IL-4.

In the retina, vascular repair and neovascularization are performed largely by circulating EPCs because mature vascular endothelial cells for proliferation are limited (*Caballero et al., 2007*; *Grant et al., 2002*). EPCs are present in the bone marrow or are peripheral blood mononuclear cells (*Rohde et al., 2006*; *Schatteman and Awad, 2003*; *Schmeisser et al., 2001*), and they can differentiate into endothelial cells as late EPCs and be incorporated into the vasculature system. Alternatively, bone marrow cells will also differentiate into non-endothelial cell lineage and serve as providers of CNV-forming signals.
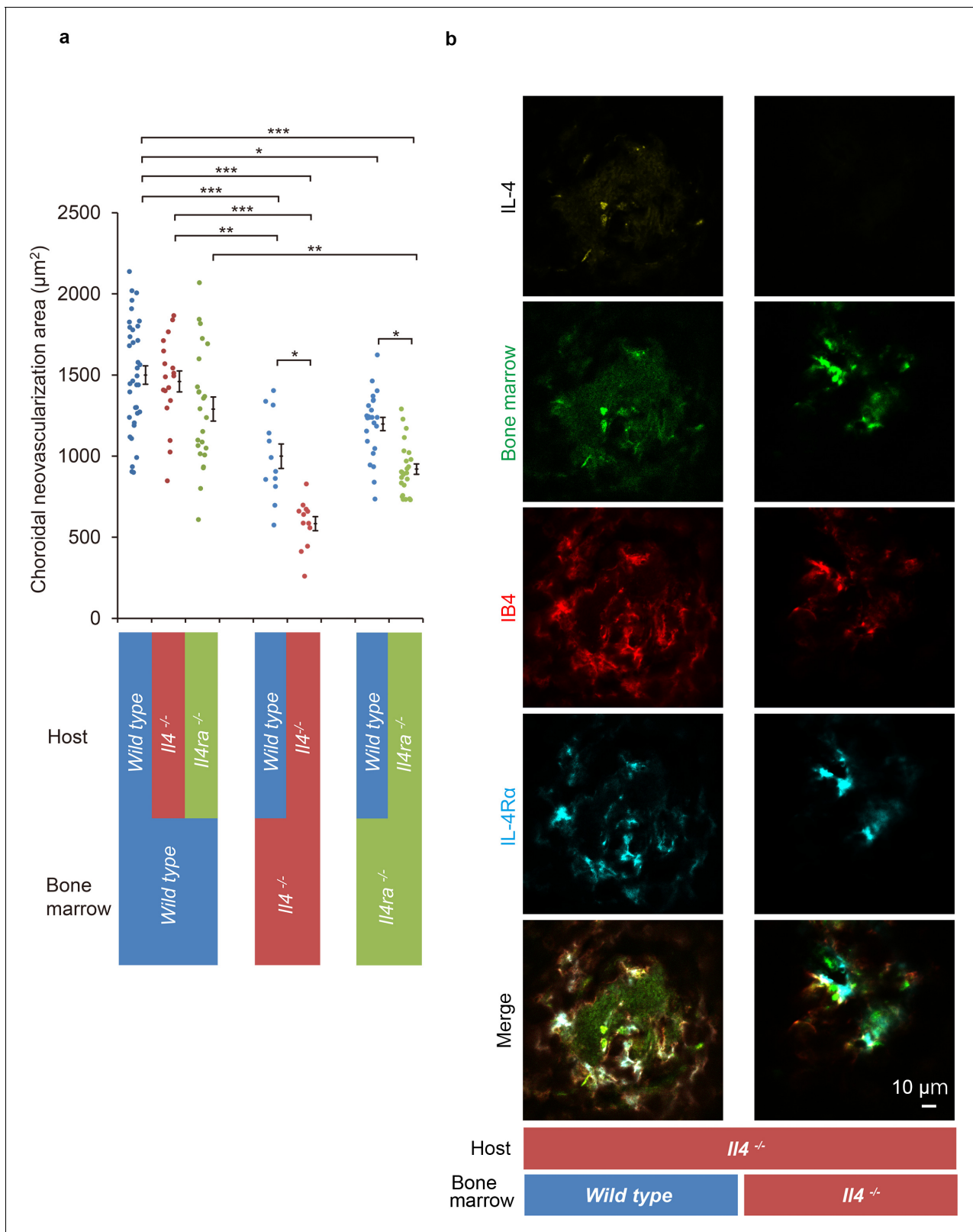
Figure 5. Role of IL-4/IL-4Rα on bone marrow-mediated choroidal neovascularization in bone marrow chimeric mice. (a) Requirement of IL-4 in bone marrow for choroidal neovascularization (CNV). Bone marrow chimeric mice were constructed on backgrounds of *wild type*, *Il4⁻/⁻*, or *Il4ra⁻/⁻* mice by transfer of *wild type Il4⁻/⁻*, or *Il4ra⁻/⁻* bone marrow cells. *Il4⁻/⁻* mice with *Il4⁻/⁻* bone marrow are most significantly impaired in CNV formation. This impairment of CNV formation is restored when bone marrow reconstituted with *wild type* bone marrow. *Il4ra⁻/⁻* mice with *Il4ra⁻/⁻* bone marrow cells are

Figure 5 continued on next page

Figure 5 continued

impaired in CNV formation. This impairment is partially restored when reconstituted with *wild type* bone marrow cells. (n = 4–12 eyes/group). Six of 10 $IL-4^{-/-}$ bone marrow chimeric mice in each group did not survive through procedures and/or were euthanized. *p<0.05, **p<0.005, ***p<0.0005. Nested ANOVA with post hoc test. (**b**) Immunohistochemical analysis of CNV of the bone marrow chimeric mice on $Il4^{-/-}$ background 14 days after laser treatment. Endothelial cells in the CNV were labeled with isolectin IB4 (red). In the $Il4^{-/-}$ mice reconstituted with *wild type* bone marrow, the CNV lesion contained IL-4 (yellow) secreting bone marrow cells (green). The IL-4Rα-positive cells (cyan) partly overlapped with bone marrow-derived cells. Scale 10 μm.

The online version of this article includes the following source data and figure supplement(s) for figure 5:

Source data 1. Requirement of IL-4 in bone marrow for CNV.
Figure supplement 1. Immunohistochemical analysis of CNV of the bone marrow chimeric mice on $Il4ra^{-/-}$ and *wild type* background 14 days after laser treatment.

In the inductive phase of CNVs, a mobilization of circulating angiogenic cells and monocyte/macrophage lineage cells begins by the early recruitment of IL-4 secreting CD11b$^+$ bone marrow cells (*Figure 1*). As a late phase phenomenon, the IL-4R$^+$ bone marrow-derived cells are incorporated into the CNV presumably as late EPCs or non-endothelial lineage cells, together with the resident cell-derived endothelial cells. We propose that the bone marrow-derived cells contribute to both phases using IL-4 as the fate determinant.

We also noted that the IL-4/IL-4Rα axis is involved in pathologic angiogenesis. For example, IL-4 induces proinflammatory phenotypes and causes vascular leakage or increased turnover of endothelial cells (*Kotowicz et al., 2004*; *Lee et al., 2010*). IL-4 stimulates human umbilical vascular endothelial cells (HUVEC) cells to induce proinflammatory cytokines including CCL2, VCAM-1, and IL-6, as a signature of global transcriptional responses (*Lee et al., 2004*). These responses appear to be a general characteristics of vascular endothelial cells including coronary arterial endothelial cells (*Skaria et al., 2016*).

To identify an endothelial lineage, we used CD31 or isolectin staining because CD31 is highly expressed on endothelial cells and is commonly used as an endothelial cell marker. However, CD31 can also be expressed on other lineage cells including T cells, B cells, dendritic cells (DCs; *Clement et al., 2014*), neutrophils, monocytes, and macrophage (*Merchand-Reyes et al., 2019*).

Our data support the idea that bone marrow-derived cells may be able to differentiate into endothelial cells in the CNV lesions. However, whether the endothelial differentiation is complete or bone marrow cells serve as immature or of different lineage was not definitively determined. Importantly, bone marrow-derived cells do play pivotal roles in the CNV formation.

In conclusion, damages of the retina and choroidal tissue release signals to the bone marrow to repair the vascular damage. This signal induces a recruitment of the bone marrow-derived cells for differentiation into or establishment of new vessels. Calling and/or fate determining signals are governed by IL-4. IL-4 may serve as a therapeutic target to treat this visual disorder.

Materials and methods

Key resources table

Reagent type (species) or resource	Designation	Source or reference	Identifiers	Additional information
Genetic reagent (*M. musculus*)	*C57BL/6J (wt)*	PMID:15729571	RRID:IMSR_JAX:000664	
Genetic reagent (*M. musculus*)	*C57BL/6-Tg (CAG-EGFP)*	PMID:9175875	RRID:IMSR_JAX:003291	
Genetic reagent (*M. musculus*)	*C57BL/6-Il4^{tm1Nnt}/J*	PMID:8906833	RRID:IMSR_JAX:002518	
Genetic reagent (*M. musculus*)	*BALB/c-Il4ra^{tm1Sz}/J*	PMID:9380721	RRID:IMSR_JAX:003514	

Continued on next page

Continued

Reagent type (species) or resource	Designation	Source or reference	Identifiers	Additional information
Genetic reagent (*M. musculus*)	*Il13ra1^tm1Twy*	PMID:18066066	RRID:MGI:3772446	Dr. Marc E Rothenberg, Cincinnati Children's Hospital Medical Center University of Cincinnati College of Medicine
Cell line (*M. musculus*)	*C57BL/6* Mouse Primary Retinal Microvascular Endothelial Cells	Cell Biologics	C57-6065	
Cell line (*H. sapiens*)	Primary Human Retinal Microvascular Endothelial Cells	Cell Systems	ACBRI 181	
Antibody	anti IL-4 (rat monoclonal)	Biolegend	Cat. #: 504108, RRID:AB_315322	IHC(1:200)
Antibody	anti IL-4 (rabbit polyclonal)	abcam	Cat. #: ab9622, RRID:AB_308736	IHC(1:200)
Antibody	anti Phospho-Tyr497 IL-4R/CD124 (rabbit polyclonal)	Assay Biotechnology Company	Cat. #: A1064, RRID:AB_10683571	IHC(1:200)
	anti CD124 (rat monoclonal)	BD Pharmingen	Cat. #: 552288, RRID:AB_394356	0.1–10 ng/ mL TVI
Antibody	anti IL-13 receptor alpha 1 (rabbit polyclonal)	abcam	Cat. #: ab-79277, RRID:AB_1640587	IHC(1:200)
	anti IL13 antibody (rabbit polyclonal)	GeneTex, Inc	Cat. #: GTX59763,	0.1–10 ng/ mL TVI
Antibody	anti CD11b (rat monoclonal)	eBioscience	Cat. #: 14-0112-82, RRID:AB_467108	IHC(1:200)
Antibody	anti CD11b (rat monoclonal) Alexa Fluor 594	Biolegend	Cat. #: 101254, RRID:AB_2563231	IHC(1:100)
Antibody	CD11b (M1/70) (rat monoclonal) FITC	eBioscience	Cat. #: 11-0112-41, RRID:AB_11042156	IHC(1:100)
Antibody	anti CCR2 (rabbit polyclonal) DyLight 550	Novus Biologicals	Cat. #: NBP1-48338R	IHC(1:100)
Antibody	anti MCP-1 (hamster monoclonal)	Biolegend	Cat. #: 505906, RRID:AB_2071552	IHC(1:200)
Antibody	anti Iba1 (rabbit polyclonal)	FUJIFILM Wako Pure Chemical Corporation	Cat. # 019–19741, RRID:AB_839504	IHC(1:200)
Antibody	anti CD31 (rabbit polyclomal)	abcam	Cat. #: ab28364, RRID:AB_726362	IHC(1:200)
Antibody	anti-mouse CD31(rat monoclonal) Alexa Fluor 647	Biolegend	Cat. #: 102516, RRID:AB_2161029	IHC(1:100)
Antibody	anti rat IgG (goat polyclonal) Brilliant Violet 421	Biolegend	Cat. #: 405414, RRID:AB_10900808	IHC(1:100)
Antibody	anti rabbit IgG (goat polyclonal) DyLight 488	Vector Laboratories	Cat. #: DI-1488, RRID:AB_2336402	IHC(1:100)
Antibody	anti rabbit IgG (donkey polyclonal) Alexa Fluor 555	Biolegend	Cat. #: 406412, RRID:AB_2563181	IHC(1:100)

Continued on next page

Continued

Reagent type (species) or resource	Designation	Source or reference	Identifiers	Additional information
Antibody	anti rabbit IgG (goat polyclonal) HiLyte Fluor 555	AnaSpec	Cat. #: AS-61056–05 H555	IHC(1:100)
Antibody	anti hamster IgG (goat polyclonal) DyLight 594	Biolegend	Cat. #: 405504, RRID:AB_1575119	
Antibody	anti rabbit IgG (goat polyclonal) PE	Santa Cruz Biotechnology	Cat. #: sc-3739, RRID:AB_649004	IHC(1:100)
Antibody	anti rabbit IgG (donkey polyclonal) Alexa Fluor 647	abcam	Cat. #: ab150075, RRID:AB_2752244	IHC(1:100)
Antibody	anti rabbit IgG (donkey polyclonal) DyLight 649	Biolegend	Cat. #: 406406, RRID:AB_1575135	IHC(1:100)
Antibody	anti mouse IgG2A (rat monoclonal)	R and D	Cat. #: mab006, RRID:AB_357349	0.1–10 ng/ mL TVI
Antibody	anti mouse Fc gamma RII/RIII (CD32/CD16)(goat polyclonal)	R and D	Cat. #: AF1460-SP, Accession # P08101	IHC (0.2 µg/mL)
Peptide, recombinant protein	recombinant murine IL-4	R and D	Cat. #: 404 ML	
Peptide, recombinant protein	recombinant human IL-4	Peprotec	Cat. #: AF-200–04	
Peptide, recombinant protein	recombinant murine IL-13	Peprotec	Cat. #: 210–13	
Chemical compound, drug	ZM306416 hydrochloride	abcam	Cat. #: ab144576	
Chemical compound, drug	ZM323881 hydrochloride	R and D	Cat. #: 2475/1	
Chemical compound, drug	bovine serum albumin	Sigma-Aldrich	Cat. #: A2153	
Chemical compound, drug	fetal bovine serum	Sigma-Aldrich	Cat. #: 12103C	
Chemical compound, drug	Medetomidine	Chemscene LLC	Cat. #: 86347-14-0	
Chemical compound, drug	Butorphanol tartrate	FUJIFILM Wako Pure Chemical Corporation	Cat. #: 58786-99-5	
Chemical compound, drug	Midazolam	FUJIFILM Wako Pure Chemical Corporation	Cat. #: 59467-70-8	
Chemical compound, drug	Tropicamide, Phenylephrine Hydrochloride	Santen Pharmaceutical Co., Ltd.	Cat. #: 1319810Q1053	

Continued on next page

Continued

Reagent type (species) or resource	Designation	Source or reference	Identifiers	Additional information
Chemical compound, drug	Hydroxy methyl cellulose	SENJU Pharmaceutical Co.,Ltd	Cat.#: 131980AQ1038	
Chemical compound, drug	RNAlater solution	Ambion	Cat. #: AM7021	
Chemical compound, drug	Triton X-100	Sigma-Aldrich	Cat. #: X100 100ml	
Chemical compound, drug	Tween 20	Sigma-Aldrich	Cat. #: P1379-100ml	
Chemical compound, drug	Paraformadehyde	Electron Microscopy Science	Cat. #: 15710	
Commercial assay or kit	ISOLECTIN B4 Fluorescein	Vector Laboratories	Cat. #: FL-1201, RRID:AB_2314663	IHC(1:100)
Commercial assay or kit	ISOLECTIN B4 DyLight 594	Vector Laboratories	Cat. #: FL-1207	IHC(1:100)
Commercial assay or kit	DAPI	Roche Diagnostics	Cat. #: 10 236 276 001	1 µg/ml
Commercial assay or kit	TO-PRO-3 iodide	Molecular Probes, Inc	Cat. #: T-3605	IHC(1:100)
Commercial assay or kit	VECTASHIELDAntifade Mounting Medium	Vector Laboratories	Cat. #: H-1000, RRID:AB_2336789	
Commercial assay or kit	Fluorescence Mounting Medium	DAKO	Cat. #: 15710	
Commercial assay or kit	SurePrint G3 Mouse GE 8 × 60K Microarray	Agilent Technologies	Cat. #: AGLMO002	
Commercial assay or kit	QuantiTect Reverse Transcription Kit	Qiagen	Cat. #: 205311	
Commercial assay or kit	QuantiTect SYBR Green PCR kit	Qiagen	Cat. #: 204143	
Commercial assay or kit	ELISA kits	ThermoFisher Scientific	Cat. #: BMS6005, EMFLT1	
Commercial assay or kit	PKH26 Red Fluorescent Cell Linker Kit for General Cell Membrane Labeling	Sigma-Aldrich	Cat. #: PKH26GL-1KT	
Commercial assay or kit	RNeasy Mini Kit	Qiagen	Cat. #: 74104	
Commercial assay or kit	DMEM:F12	ThermoFisher Scientific	Cat. #: 11330057	
Commercial assay or kit	recombinant human GMCSF	Peprotec	Cat. #: AF-300–03	
Commercial assay or kit	recombinant murine GMCSF	Peprotec	Cat. #: 315–03	
Software, algorithm	Ingenuity Pathway Analysis, March 2020	Qiagen	RRID:SCR_008653	
Software, algorithm	Adobe Photoshop CS5, Version 12.0.5	Adobe	RRID:SCR_014199	
Software, algorithm	STATA 16.1	StataCorp LLC	RRID:SCR_012763	
Software, algorithm	GeneSpring Software	Agilent Technologies	RRID:SCR_009196	

Patient selection and measurement of aqueous humor IL-4

The diagnosis of AMD and subtypes of AMD including PCV and RAP was made by the clinical characteristics. The presence of a CNV or retinal angiomatous proliferation (RAP) was determined by fluorescein angiography, indocyanine green angiography, and spectral domain optical coherence tomography (SD-OCT).

The inclusion criteria were the presence of active CNVs or RAP lesions determined by the angiographic images showing macular edema or subfoveal hemorrhages. Eyes with laser photocoagulation, photodynamic therapy, or intraocular surgery within the past 3 months were excluded. For the control groups, aqueous humor was collected from normal patients who were undergoing routine cataract surgery.

The levels of IL-4 and IL-13 in the aqueous humor samples were measured by commercial ELISA kits as described in detail (*Chono et al., 2018*; *Sasaki et al., 2012*).

Animals

Il4-deficient mice, C57BL/6-*Il4*^{tm1Nnt}/J, *Il4ra*-deficient mice, and BALB/c-*Il4ra*^{tm1Sz}/J, were obtained from The Jackson Laboratory (Bar Harbor, ME). The *Il4ra*-deficient mice were backcrossed with C57BL/6 for 9 generations. The *Il13ra1*-deficient mice were obtained from the Regeneron Pharmaceuticals (Tarrytown, NY). *Green fluorescent protein* (*GFP*) transgenic C57BL/6 and *wild type* C57BL/6 mice were purchased from Japan SLC Inc (Shizuoka, Japan).

Induction of choroidal neovascularization

Choroidal neovascularization (CNV) was induced by laser irradiation of the retina of mice, an established model for choroidal or retinal neovascular formation. This model has many characteristics of age-related macular degeneration. Mice were anesthetized and one eye was exposed to argon laser irradiation of 150 mW for 0.10 s. Three laser spots were created in each eye. The spot size was approximately 50 μm, and it was delivered with the Novus 2000 argon laser system (Coherent, Santa Clara, CA).

To analyze the CNVs, the laser-treated eyes were enucleated from euthanized mice 14 days after the photocoagulation. Choroidal sheets were isolated from the eyes and fixed in 4% paraformaldehyde at 4° C for 1 min. The choroidal sheets were stained with FITC or DyLight 594 conjugated Isolectin IB4 (Vector Laboratories, Peterborough, UK) and flat-mounted. The stained flat mounts sections were examined and photographed with a fluorescence stereo microscope (MZ-III, Leica Microsystems, Wetzlar, Germany). The isolectin IB4 reactive areas were analyzed as the CNV area by masked investigators to measure the CNV size.

Immunohistochemistry of choroidal neovascularization

For the immunohistochemical analyses of the CNVs, isolated choroidal sheets with or without the retina were fixed in 4% paraformaldehyde and incubated with isolectin IB4 and primary antibodies including anti-IL-4 (11B11, Biolegend, San Diego, CA), anti-IL-4Rα (mIL4R-M1, BD Biosciences, Franklin Lakes, NJ), anti-Iba1 (FUJIFILM, Tokyo, Japan), anti-IL-13R (ab-79277, abcam, Cambridge, UK), anti-CD11b (M1/70, eBioscience, San Diego, CA), anti-CCL2 (2H5, Biolegend), anti-CCR2 (NBP1-48338R, Novus Biologicals, Centennial, CO), or anti-CD31 (390, Biolegend) with anti-Fc RII/RIII blocking antibody (R and D Systems, McKinley Place, NE) overnight at 4° C. Then, the choroidal sheets were rinsed and incubated with the secondary antibodies labeled with either Brilliant Violet 421, DyLight 488, Alexa Fluor 555, PE, Alexa Fluor 647, or DyLight 649, or control antibodies. DAPI and TO-PRO-3 iodide (T-3605, Molecular Probes, Eugene, OR) were used for nuclear staining. A confocal microscope (LSM730, Carl Zeiss, Oberkochen, Germany), or a fluorescence microscope (BZ-X800, Keyence, Osaka, Japan) was used for photographing the whole mounts.

Intravenous injection of IL-4/IL-13 and blockade by antibody

After the laser irradiation, recombinant mouse IL-4 (R and D Systems, Minneapolis, MN), IL-13 (Peprotec, Rocky Hill, NJ), or vehicle was injected through a tail vein on days 0 and 3. To block the induction of IL-4 or IL-13, anti-IL4 antibody (50 μg/mouse, BioLegend), anti-IL13 antibody (50 μg/mouse, Gene Tex, Irvine, CA), or control IgG was injected through the tail vein on days 0 and 3.

Generation of bone marrow chimeric mice

Bone marrow cells were collected from the femur and tibia as described in detail (*Wu et al., 2015*). Recipient mice were irradiated (600 rad × 2) with a MX-160Labo Irradiator (MediXtec, Chiba, Japan) and then injected with a bone marrow cell suspension (1 × 10⁷ cells) through the tail vein. The transplanted mice were allowed to recover for 5 weeks to reconstitute their myeloid cells. The reconstitution was confirmed by flow cytometry and the staining of the bone marrow or blood samples.

GFP transgenic mice-derived bone marrow or PKH26 (Sigma, Saint Louis, MO) labeling was used to examine the bone marrow cells. The stability of the PKH labeling was examined in the chimeric mice transplanted with PKH-labeled *GFP*-transgenic bone marrow. A stable co-localization of PKH and GFP in the bone marrow cells for more than 6 weeks was confirmed (data not shown).

Real-time reverse transcription PCR (RT-PCR)

The eyes of laser-irradiated mice were enucleated at the selected times after the photocoagulation. Total RNA was extracted from the retina and choroidal sheets with the RNeasy mini kit (Qiagen, Hilden, Germany) and transcribed using the QuantiTect Reverse Transcription Kit (Qiagen). The cDNAs were amplified with QuantiTect SYBR Green PCR kit (Qiagen) with primer pairs (*Supplementary file 1*), and quantified using the LightCycler (Roche, Mannheim, Germany).

Retinal microvascular endothelial cells and endothelial progenitor cells

Primary retinal vascular endothelial cells were collected from murine (C57-6065, Cell Biologics, Chicago, IL) and human retinas (ACBRI 181, Cell Systems, Kirkland, WA).

Primary retinal microvascular endothelial cells of *C57BL/6* mice were isolated from the retinal tissue of pathogen-free laboratory mice. The cells were negative for bacteria, yeast, fungi, and mycoplasma. Primary human retinal microvascular endothelial cells were also examined for absence of human immunodeficiency virus (HIV), hepatitis B virus (HBV), and hepatitis C virus (HCV) contaminations by serologic or PCR test (by CLIA Licensed Clinical Lab) and *Mycoplasma* spp. contaminations (ATCC method by CLIA Licensed Clinical Lab). They were propagated to confluence on gelatin-coated 96-well plates in Dulbecco's modified Eagle's medium (DMEM; Gibco, Grand Island, NY) supplemented with 10% fetal bovine serum, L-glutamine, endothelial cell growth supplement (Sigma, St. Louis, MO), heparin, and non-essential amino acids (Gibco).

To create endothelial progenitor cells (EPCs), isolated bone marrow cells of mice were plated on fibronectin-coated plates. The nonadherent cells were removed, and the attached cells were cultured for 2 weeks in DME/F-12 supplement with 15% FBS and recombinant GMCSF (10 ng/ml, Peprotec, Rocky Hill, NJ) (*Wang et al., 1998*). Colony forming units were formed and attached at 1 week. To confirm an endothelial cell lineage, the cells were stained with endothelial cell markers including CD31, VCAM-1, and von Willebrand factor. Briefly, cells plated on temperature-responsive dishes (CellSeed, Tokyo, Japan) were non-enzymatically dispersed and stained for FACS analysis.

Tube formation assay of endothelial cells and microarray analysis

To examine the roles played by cytokines in angiogenesis, vascular endothelial cells were assayed for in vitro tube formation as described in detail (*DeCicco-Skinner et al., 2014*). Briefly, bone marrow-derived EPCs or retinal vascular endothelial cells were plated on Matrigel-coated plates with or without recombinant mouse IL-4 (R and D Systems) or recombinant human IL-4 (Peprotec, for human endothelial cells), and the presence of tube networks was quantified by digitization of the photographs by Photoshop (Adobe, San Jose, CA) after 24 hr.

The gene and the pathway associated with the tube formation were determined by microarray analysis of tube forming EPCs. EPCs derived from *wild type* or *Il4ra⁻ᐟ⁻* mice were plated on Matrigel plates with or without IL-4 (10 ng/ml) to examine for tube formation. The total RNA was extracted using RNeasy mini kit (Qiagen) and analyzed using SurePrint G3 Mouse GE 8 × 60K Microarray (Agilent Technologies, Santa Clara, CA) (*Miyazaki et al., 2017*). The microarray data were analyzed using GeneSpring Software with setting of single color array and a fold change cut off of 3 and a $p<0.05$. A set of the IL-4-induced genes in the bone marrow-derived EPCs was analyzed to identify the canonical pathways and upstream regulators using Ingenuity Pathway Analysis software (IPA, Qiagen, accessed on 2020/4/5). The transcriptional networks of IL-4-stimulated EPCs were also

constructed using IPA and evaluated by the *P* value as likelihood that assembly of the genes in a network could be explained by random chance alone.

Enzyme-linked immunosorbent assay (ELISA)

The supernatants of EPC were assayed with a commercial ELISA kit (ThermoFisher Scientific, Waltham MA). The levels of IL-4 and IL-13 in the aqueous humor samples were measured using commercial ELISA kit as described in detail (*Chono et al., 2018*; *Sasaki et al., 2012*).

Statistical analyses

Data are presented as the means ± standard error of the means (SEMs). The significance of the differences was determined by two-tailed *t* tests, linear mixed-effects regression analysis, or ANOVA with post hoc tests. Logistic regression analysis was used to compute the odds ratios based on quintiles of each cytokine levels. A $p < 0.05$ was taken to be significant.

Additional information

Competing interests

Yoshitsugu Inoue: medical advisor of Senju Pharmaceutical Company, Japan. The other authors declare that no competing interests exist.

Author contributions

Takashi Baba, Conceptualization, Data curation, Formal analysis, Funding acquisition, Investigation, Writing - original draft, Writing - review and editing; Dai Miyazaki, Conceptualization, Data curation, Software, Formal analysis, Supervision, Writing - original draft, Project administration, Writing - review and editing; Kodai Inata, Ryu Uotani, Hitomi Miyake, Shin-ichi Sasaki, Yumiko Shimizu, Data curation, Formal analysis, Investigation; Yoshitsugu Inoue, Supervision, Funding acquisition, Project administration, Writing - review and editing; Kazuomi Nakamura, Resources, Formal analysis, Supervision, Methodology

Author ORCIDs

Takashi Baba https://orcid.org/0000-0001-7318-9420

Ethics

Human subjects: The study protocol was approved by the Ethics Committee of the Tottori University (protocol #: 2699), and the procedures used conformed to the tenets of the Declaration of Helsinki. An informed consent was obtained from all of the participants.

Animal experimentation: All mice were handled in accordance with the ARVO Statement for the Use of Animals in Ophthalmic and Vision Research and protocols approved by the Institutional Animal Care and Use Committee of Tottori University (protocol #: 12-Y-7, 13-Y-25, 16-Y-22, and 19-Y-50).

Decision letter and Author response
Decision letter https://doi.org/10.7554/eLife.54257.sa1
Author response https://doi.org/10.7554/eLife.54257.sa2

Additional files
Supplementary files
• Supplementary file 1. Sequences of primer pairs used in quantitative reverse-transcription polymerase chain reaction.

• Transparent reporting form

Data availability
All data generated or analysed during this study are included in the manuscript. Source data files have been provided for Figure 1, 2, 3, Figure 3—figure supplement 1, 2, Figure 4, Figure 4—figure supplement 1 and Figure 5.

References

Adão-Novaes J, Guterres CC, da Silva AG, Campello-Costa P, Linden R, Sholl-Franco A. 2009. Interleukin-4 blocks thapsigargin-induced cell death in rat rod photoreceptors: involvement of cAMP/PKA pathway. *Journal of Neuroscience Research* **87**:2167–2174. DOI: https://doi.org/10.1002/jnr.22026, PMID: 19235892

Antonioli L, Blandizzi C, Pacher P, Guilliams M, Haskó G. 2018. Quorum sensing in the immune system. *Nature Reviews Immunology* **18**:537–538. DOI: https://doi.org/10.1038/s41577-018-0040-4, PMID: 30006523

Beck M, Munk MR, Ebneter A, Wolf S, Zinkernagel MS. 2016. Retinal ganglion cell layer change in patients treated with Anti-Vascular endothelial growth factor for neovascular Age-related macular degeneration. *American Journal of Ophthalmology* **167**:10–17. DOI: https://doi.org/10.1016/j.ajo.2016.04.003, PMID: 270 84000

Caballero S, Sengupta N, Afzal A, Chang KH, Li Calzi S, Guberski DL, Kern TS, Grant MB. 2007. Ischemic vascular damage can be repaired by healthy, but not diabetic, endothelial progenitor cells. *Diabetes* **56**:960–967. DOI: https://doi.org/10.2337/db06-1254, PMID: 17395742

Cao X, Shen D, Patel MM, Tuo J, Johnson TM, Olsen TW, Chan CC. 2011. Macrophage polarization in the maculae of age-related macular degeneration: a pilot study. *Pathology International* **61**:528–535. DOI: https://doi.org/10.1111/j.1440-1827.2011.02695.x, PMID: 21884302

Chen CC, Wang L, Plikus MV, Jiang TX, Murray PJ, Ramos R, Guerrero-Juarez CF, Hughes MW, Lee OK, Shi S, Widelitz RB, Lander AD, Chuong CM. 2015. Organ-level quorum sensing directs regeneration in hair stem cell populations. *Cell* **161**:277–290. DOI: https://doi.org/10.1016/j.cell.2015.02.016, PMID: 25860610

Chitnis T, Weiner HL. 2017. CNS inflammation and neurodegeneration. *Journal of Clinical Investigation* **127**:3577–3587. DOI: https://doi.org/10.1172/JCI90609, PMID: 28872464

Chono I, Miyazaki D, Miyake H, Komatsu N, Ehara F, Nagase D, Kawamoto Y, Shimizu Y, Ideta R, Inoue Y. 2018. High interleukin-8 level in aqueous humor is associated with poor prognosis in eyes with open angle Glaucoma and neovascular Glaucoma. *Scientific Reports* **8**:14533. DOI: https://doi.org/10.1038/s41598-018-32725-3, PMID: 30266980

Clement M, Fornasa G, Guedj K, Ben Mkaddem S, Gaston AT, Khallou-Laschet J, Morvan M, Nicoletti A, Caligiuri G. 2014. CD31 is a key coinhibitory receptor in the development of immunogenic dendritic cells. *PNAS* **111**:E1101–E1110. DOI: https://doi.org/10.1073/pnas.1314505111, PMID: 24616502

Copland DA, Theodoropoulou S, Liu J, Dick AD. 2018. A perspective of AMD through the eyes of immunology. *Investigative Opthalmology & Visual Science* **59**:amd83–amd92. DOI: https://doi.org/10.1167/iovs.18-23893

da Silva AG, Campello-Costa P, Linden R, Sholl-Franco A. 2008. Interleukin-4 blocks proliferation of retinal progenitor cells and increases rod photoreceptor differentiation through distinct signaling pathways. *Journal of Neuroimmunology* **196**:82–93. DOI: https://doi.org/10.1016/j.jneuroim.2008.03.003, PMID: 18378323

DeCicco-Skinner KL, Henry GH, Cataisson C, Tabib T, Gwilliam JC, Watson NJ, Bullwinkle EM, Falkenburg L, O'Neill RC, Morin A, Wiest JS. 2014. Endothelial cell tube formation assay for the in vitro study of angiogenesis. *Journal of Visualized Experiments*:e51312. DOI: https://doi.org/10.3791/51312, PMID: 25225985

Feng C, Wang X, Liu T, Zhang M, Xu G, Ni Y. 2017. Expression of CCL2 and its receptor in activation and migration of microglia and monocytes induced by photoreceptor apoptosis. *Molecular Vision* **23**:765–777. PMID: 29142497

Gao F, Hou H, Liang H, Weinreb RN, Wang H, Wang Y. 2016. Bone marrow-derived cells in ocular neovascularization: contribution and mechanisms. *Angiogenesis* **19**:107–118. DOI: https://doi.org/10.1007/s10456-016-9497-6, PMID: 26880135

Grant MB, May WS, Caballero S, Brown GA, Guthrie SM, Mames RN, Byrne BJ, Vaught T, Spoerri PE, Peck AB, Scott EW. 2002. Adult hematopoietic stem cells provide functional hemangioblast activity during retinal neovascularization. *Nature Medicine* **8**:607–612. DOI: https://doi.org/10.1038/nm0602-607, PMID: 12042812

Grochot-Przeczek A, Kozakowska M, Dulak J, Jozkowicz A. 2013.Dulak J, Józkowicz A, Łoboda A (Eds). *Angiogenesis and Vascularisation: Cellular and Molecular Mechanisms in Health and Diseases*. Wien: Springer-Verlag. DOI: https://doi.org/10.1007/978-3-7091-1428-5

Haas CS, Amin MA, Allen BB, Ruth JH, Haines GK, Woods JM, Koch AE. 2006. Inhibition of angiogenesis by interleukin-4 gene therapy in rat adjuvant-induced arthritis. *Arthritis & Rheumatism* **54**:2402–2414. DOI: https://doi.org/10.1002/art.22034, PMID: 16869003

Kiyota T, Okuyama S, Swan RJ, Jacobsen MT, Gendelman HE, Ikezu T. 2010. CNS expression of anti-inflammatory cytokine interleukin-4 attenuates alzheimer's disease-like pathogenesis in APP+PS1 bigenic mice. *The FASEB Journal* **24**:3093–3102. DOI: https://doi.org/10.1096/fj.10-155317, PMID: 20371618

Koeberle PD, Gauldie J, Ball AK. 2004. Effects of adenoviral-mediated gene transfer of interleukin-10, interleukin-4, and transforming growth factor-beta on the survival of axotomized retinal ganglion cells. *Neuroscience* **125**:903–920. DOI: https://doi.org/10.1016/S0306-4522(03)00398-1, PMID: 15120851

Kotowicz K, Callard RE, Klein NJ, Jacobs MG. 2004. Interleukin-4 increases the permeability of human endothelial cells in culture. *Clinical Experimental Allergy* **34**:445–449. DOI: https://doi.org/10.1111/j.1365-2222.2004.01902.x, PMID: 15005739

Lee YW, Eum SY, Chen KC, Hennig B, Toborek M. 2004. Gene expression profile in interleukin-4-stimulated human vascular endothelial cells. *Molecular Medicine* **10**:19–27. DOI: https://doi.org/10.2119/2004-00024.Lee, PMID: 15502879

Lee YW, Kim PH, Lee WH, Hirani AA. 2010. Interleukin-4, oxidative stress, vascular inflammation and atherosclerosis. *Biomolecules and Therapeutics* **18**:135–144. DOI: https://doi.org/10.4062/biomolther.2010.18.2.135, PMID: 21072258

Leung KW, Barnstable CJ, Tombran-Tink J. 2009. Bacterial endotoxin activates retinal pigment epithelial cells and induces their degeneration through IL-6 and IL-8 autocrine signaling. *Molecular Immunology* **46**:1374–1386. DOI: https://doi.org/10.1016/j.molimm.2008.12.001, PMID: 19157552

Lückoff A, Caramoy A, Scholz R, Prinz M, Kalinke U, Langmann T. 2016. Interferon-beta signaling in retinal mononuclear phagocytes attenuates pathological neovascularization. *EMBO Molecular Medicine* **8**:670–678. DOI: https://doi.org/10.15252/emmm.201505994, PMID: 27137488

Merchand-Reyes G, Robledo-Avila FH, Buteyn NJ, Gautam S, Santhanam R, Fatehchand K, Mo X, Partida-Sanchez S, Butchar JP, Tridandapani S. 2019. CD31 acts as a checkpoint molecule and is modulated by FcγR-Mediated signaling in monocytes. *The Journal of Immunology* **203**:3216–3224. DOI: https://doi.org/10.4049/jimmunol.1900059, PMID: 31732534

Miyazaki D, Uotani R, Inoue M, Haruki T, Shimizu Y, Yakura K, Yamagami S, Suzutani T, Hosogai M, Isomura H, Inoue Y. 2017. Corneal endothelial cells activate innate and acquired arm of anti-viral responses after Cytomegalovirus infection. *Experimental Eye Research* **161**:143–152. DOI: https://doi.org/10.1016/j.exer.2017.06.017, PMID: 28648760

Pearson JD. 2010. Endothelial progenitor cells–an evolving story. *Microvascular Research* **79**:162–168. DOI: https://doi.org/10.1016/j.mvr.2009.12.004, PMID: 20043930

Rohde E, Malischnik C, Thaler D, Maierhofer T, Linkesch W, Lanzer G, Guelly C, Strunk D. 2006. Blood monocytes mimic endothelial progenitor cells. *Stem Cells* **24**:357–367. DOI: https://doi.org/10.1634/stemcells.2005-0072, PMID: 16141361

Sasaki M, Miyakoshi M, Sato Y, Nakanuma Y. 2010. Modulation of the microenvironment by senescent biliary epithelial cells may be involved in the pathogenesis of primary biliary cirrhosis. *Journal of Hepatology* **53**:318–325. DOI: https://doi.org/10.1016/j.jhep.2010.03.008, PMID: 20570384

Sasaki S, Miyazaki D, Miyake K, Terasaka Y, Kaneda S, Ikeda Y, Funakoshi T, Baba T, Yamasaki A, Inoue Y. 2012. Associations of IL-23 with polypoidal choroidal vasculopathy. *Investigative Opthalmology & Visual Science* **53**:3424–3430. DOI: https://doi.org/10.1167/iovs.11-7913

Schatteman GC, Awad O. 2003. In vivo and in vitro properties of CD34+ and CD14+ endothelial cell precursors. *Advances in Experimental Medicine and Biology* **522**:9–16. DOI: https://doi.org/10.1007/978-1-4615-0169-5_2, PMID: 12674206

Schmeisser A, Garlichs CD, Zhang H, Eskafi S, Graffy C, Ludwig J, Strasser RH, Daniel WG. 2001. Monocytes coexpress endothelial and macrophagocytic lineage markers and form cord-like structures in matrigel under angiogenic conditions. *Cardiovascular Research* **49**:671–680. DOI: https://doi.org/10.1016/S0008-6363(00)00270-4, PMID: 11166280

Sennlaub F, Auvynet C, Calippe B, Lavalette S, Poupel L, Hu SJ, Dominguez E, Camelo S, Levy O, Guyon E, Saederup N, Charo IF, Rooijen NV, Nandrot E, Bourges JL, Behar-Cohen F, Sahel JA, Guillonneau X, Raoul W, Combadiere C. 2013. CCR2(+) monocytes infiltrate atrophic lesions in age-related macular disease and mediate photoreceptor degeneration in experimental subretinal inflammation in *Cx3cr1* deficient mice. *EMBO Molecular Medicine* **5**:1775–1793. DOI: https://doi.org/10.1002/emmm.201302692, PMID: 24142887

Skaria T, Burgener J, Bachli E, Schoedon G. 2016. IL-4 causes hyperpermeability of vascular endothelial cells through Wnt5A signaling. *PLOS ONE* **11**:e0156002. DOI: https://doi.org/10.1371/journal.pone.0156002, PMID: 27214384

Volpert OV, Fong T, Koch AE, Peterson JD, Waltenbaugh C, Tepper RI, Bouck NP. 1998. Inhibition of angiogenesis by interleukin 4. *Journal of Experimental Medicine* **188**:1039–1046. DOI: https://doi.org/10.1084/jem.188.6.1039, PMID: 9743522

Wang QR, Yan Y, Wang BH, Li WM, Wolf NS. 1998. Long-term culture of murine bone-marrow-derived endothelial cells. *In Vitro Cellular & Developmental Biology - Animal* **34**:443–446. DOI: https://doi.org/10.1007/s11626-998-0075-0, PMID: 9661045

Wu WK, Georgiadis A, Copland DA, Liyanage S, Luhmann UF, Robbie SJ, Liu J, Wu J, Bainbridge JW, Bates DO, Ali RR, Nicholson LB, Dick AD. 2015. IL-4 regulates specific Arg-1(+) macrophage sFlt-1-mediated inhibition of angiogenesis. *The American Journal of Pathology* **185**:2324–2335. DOI: https://doi.org/10.1016/j.ajpath.2015.04.013, PMID: 26079814

Yoshida S, Yoshida A, Ishibashi T, Elner SG, Elner VM. 2003. Role of MCP-1 and MIP-1alpha in retinal neovascularization during postischemic inflammation in a mouse model of retinal neovascularization. *Journal of Leukocyte Biology* **73**:137–144. DOI: https://doi.org/10.1189/jlb.0302117, PMID: 12525571

Zhao W, Xie W, Xiao Q, Beers DR, Appel SH. 2006. Protective effects of an anti-inflammatory cytokine, interleukin-4, on motoneuron toxicity induced by activated microglia. *Journal of Neurochemistry* **99**:1176–1187. DOI: https://doi.org/10.1111/j.1471-4159.2006.04172.x, PMID: 17018025

Zhou YD, Yoshida S, Peng YQ, Kobayashi Y, Zhang LS, Tang LS. 2017. Diverse roles of macrophages in intraocular neovascular diseases: a review. *International Journal of Ophthalmology* **108**:1902–1908. DOI: https://doi.org/10.18240/ijo.2017.12.18